Supporting Information

Controlled synthesis of monodispersed ZnO nanospindles decorated TiO_2 mesospheres for enhanced charge transport in dye-sensitized solar cells

S. Athithya[a,b], S. Harish[a,b], H. Ikeda[b], M. Navaneethan[a,c] *, J. Archana[a] *

[a] Functional Materials and Energy Devices Laboratory, Department of Physics and Nanotechnology, SRM Institute of Science and Technology, Kattankulathur-603 203, Chennai, India

[b] Graduate School of Science and Technology (GSST), Shizuoka University, 3-5-1 Johoku, Naka-Ku, Hamamatsu, Shizuoka 432-8011, Japan.

[c] Nanotechnology Research Center (NRC), SRM Institute of Science and Technology, Kattankulathur-603 203, Chennai, India

Corresponding Authors

*** Dr. J. Archana**

E-mail: jayaram.archana@gmail.com

Dr. M. Navaneethan

E-mail: m.navaneethan@gmail.com

1. Fabrication of DSSC assembly

For colloidal formation, 0.25 g of prepared samples (TZC-0, TZC-0.5, TZC-0.10, TZC-0.15, TZC-0.20 and TZC-0.25) were dispersed in stock solution of ethyl cellouse and alpha terpinol grounded very well using mortal pestle for 30 min. The paste uniformly coated on the clead FTO by handmade screen-printing coating process. Then, the photoanode brought into preheat at 120 ℃ for 10 mins to prevent from cracks and pin holes during annealing process. Finally annealed at ramping temperature 450 ℃ for 30 mins. Further, the prepared photoanode soaked in ethanol solution containing 0.03 M dis-tetrabutylammonium cis-bis(isothiocyanato)bis(2,2"-bipyridyl-4,4'-dicarboxylato) ruthenium (II) (N719) for 12 h. Thereafter, prepared photoanode has attached with Pt-coated counter electrode and electrolyte solution (0.6 M dimethylpropylimidazolium iodide, 0.1 M lithium iodide, 0.01 M iodine, and 0.5 M tetrabutylpyridine in acetonitrile) filled in between photoanode and Pt cathode as a sand-wich type of cell.

2. Characterization techniques

The structural analysis has been done by X-ray diffraction (XRD using with CuKα radiation (λ= 1.5406Å), ranging between 20°-80^{o} at the scanning rate of 2^{o} per minute. The Raman vibrational spectrum of prepared sample was recorded using (JASCO-NRS-7100). The nanocomposite morphology and elemental composition was examined by FE-SEM (JEOL JSM 7001F microscope) with an accelerating voltage of 15 kV and transmission electron microscopy (JEOL JEM 2100F) at an accelerating voltage of 200 kV. The absorption and emission measurements were carried out at room temperature to analysed the optical properties of prepared sample using UV-Vis (Shimadzu, UV-2600) and photoluminescence Spectrophotometer (JASCO-FP8600). The lifetime of charge carriers was determined using time-resolved photoluminescence (TRPL: Fluorolog Spectrofluorimeter) using a 370 nm laser

as an excitation source. The porosity of the prepared samples was analysed by a Belsorp mini II instrument thru Brunauer-EmmettTeller (BET) method. X-ray photoelectron spectroscopy (XPS) was performed via a kratos analytical instrument (Shimadu Coporation, ESCA 3400, Japan) to investigate the elemental chemical states of as-prepared samples. The photovoltaic behaviour of fabricated photoanode was performed using SCIENCETECH, Canada (Class A, Lamp: 300 W). The incident photo current efficiency (IPCE) of the devices was measured using SCIENCETECH, Canada, throughout a wavelength range of 200 nm to 800 nm to acquire a better understanding. The charge carrier behaviour of the fabricated device measured using electrochemical impedance spectra (EIS) were measured with a biologic workstation (ZAHNER) with at frequency ranging from 10 mHz to 1000 kHz.

3. Growth mechanism of mesosphere TiO_2 and TiO_2/ZnO formation

The formation of mesosphere TiO_2/ZnO spindle is shown in Fig (S1). Titanium metal oxides contain moisture-sensitive alkoxide groups, So, TTIP easily hydrolyses during titania synthesis. A high hydrolysis rate results in non-uniform products, so the process must be slowed. The branched alkoxy ligands sterically inhibit hydrolysis, ethylene glycol was selected to inhibit hydrolysis via the nucleophilic substitution mechanism. According to, titania glycolate is formed when the alkoxy chain of ethylene glycol coordinates with TiO_2 nuclei according to following equation and shown in Fig. S1.

$$Ti(OCH(CH_3)_2)_4 + 2OH(CH_2)_2OH \longrightarrow Ti((OCH_2)_2)_2 + 4(CH_3)_2CHOH \text{ -----(1)}$$

The sol–gel preparation of spherical titanium glycolate precursor in acetone to control the hydrolysis and condensation reaction. The C = O functional group in acetone play an important role in the formation of monodispersed spherical titanium glycolate colloids. In addition, when 2 mL of DI water was added into acetone, it could speed up the formation of colloidal solution. Followed by solvothermal was employed to broke the coordination between the alkoxy chain

of ethylene glycolate and titania. Releasing the alkoxy group from the product will be resulted in the mesoporous TiO_2.

The formation of ZnO spindles, different molar ratio of zinc acetate mixed with DI water to form Zn^{2+} ions. Additionally, Na^+ ions from NaOH react with Zn^{2+} ions according to the following equation.

$$Zn(CH_3COO)_2(H_2O)_2+H_2O \longrightarrow Zn^{2+} + 2(CH_3COO)^- + H_2O \text{ ------- (2)}$$

$$Zn^{2+} + NaOH \longrightarrow Zn(OH)_2 + Na^+ \text{ ---------- (3)}$$

$Zn(OH)_2+Na^+$ undergoes hydrothermal reaction to produce ZnO spindles which eventually get deposited on the TiO_2 mesosphere.

$$Zn(OH)_2 \quad ZnO + H_2O \text{ ---- } \xrightarrow[\text{At annealing}]{\Delta} \quad \text{---- (4)}$$

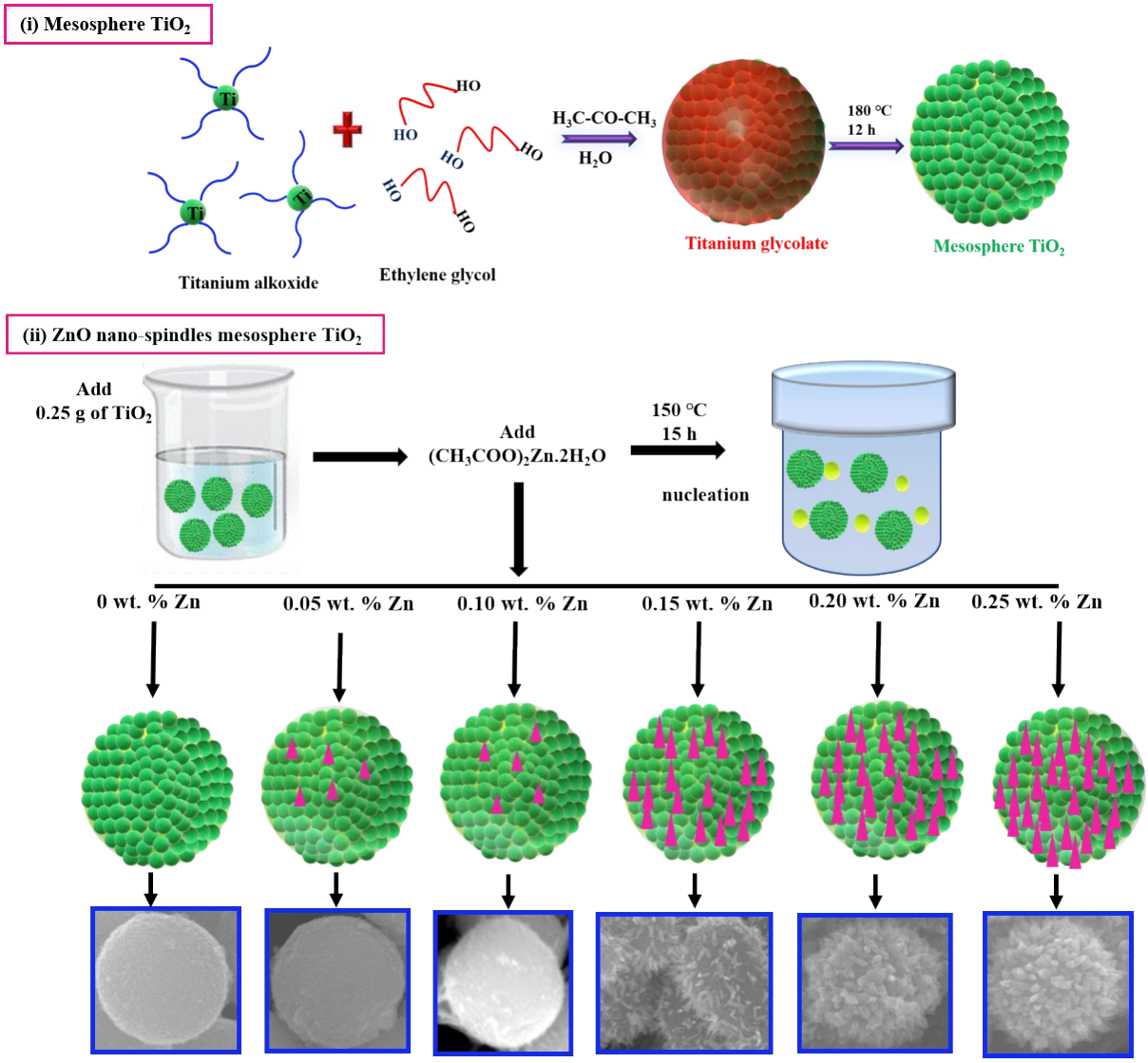

Fig S1: Possible growth mechanism of mesosphere TiO_2 and formation of ZnO spindle decorated on the mesosphere TiO_2.

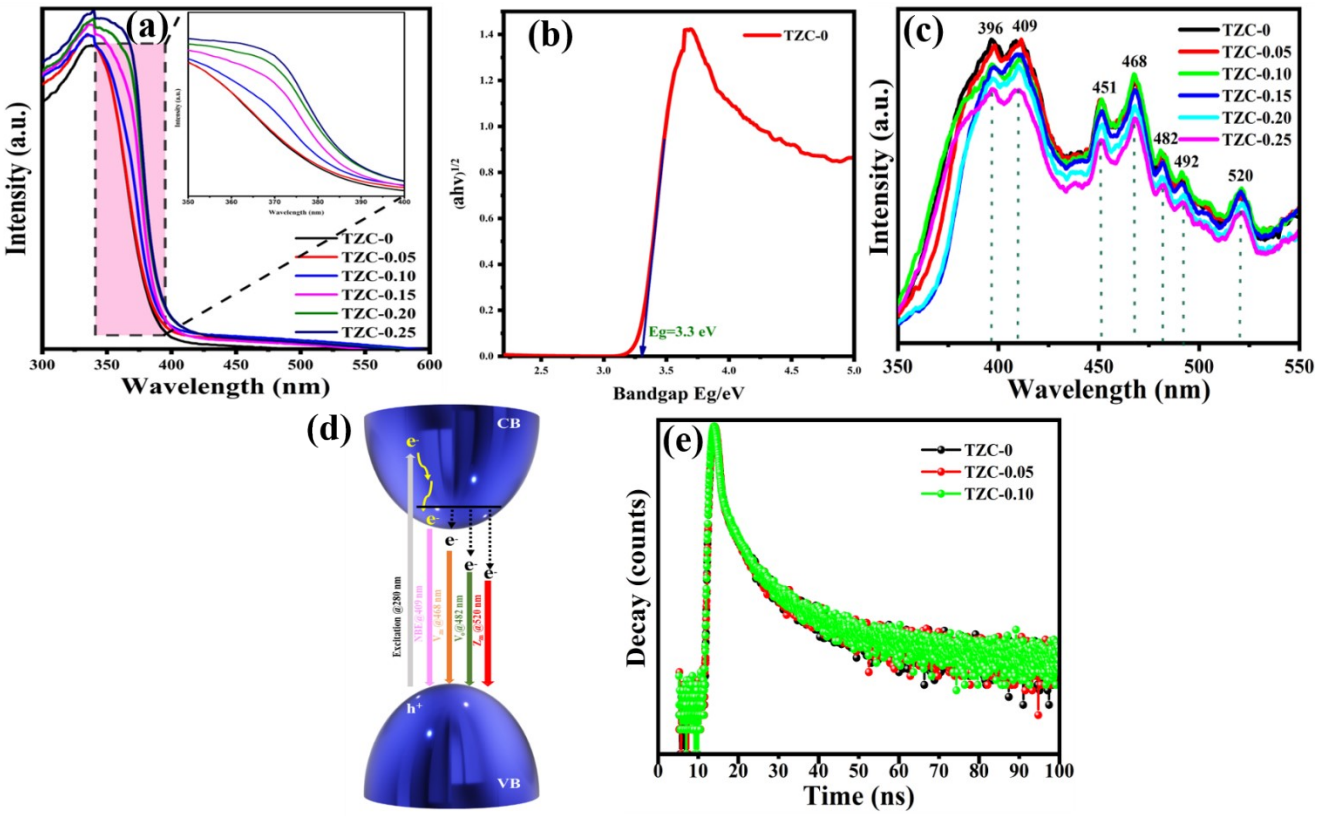

Fig S2: (a) UV-DRS spectra for TZC-0, TZC-0.05, TZC-0.10, TZC-0.15, TZC-0.20, and TZC-0.25. (b) Tauc plot of TZC-0. (c) PL Spectra for TZC-0, TZC-0.05, TZC-0.10, TZC-0.15, TZC-0.20 and TZC-0.25. (d) Depiction of possible recombination dynamics of each PL peak. and (e) TRPL spectra for TZC-0, TZC-0.05, and TZC-0.10 samples.

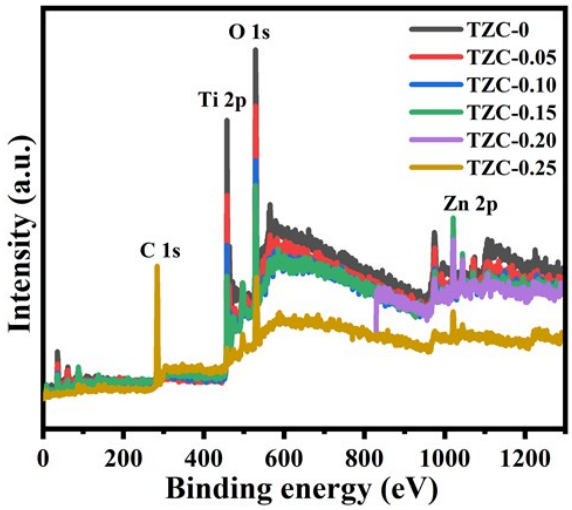

Fig S3: XPS survey spectra of prepared mesosphere TiO_2 and TiO_2/ZnO nanocomposites.

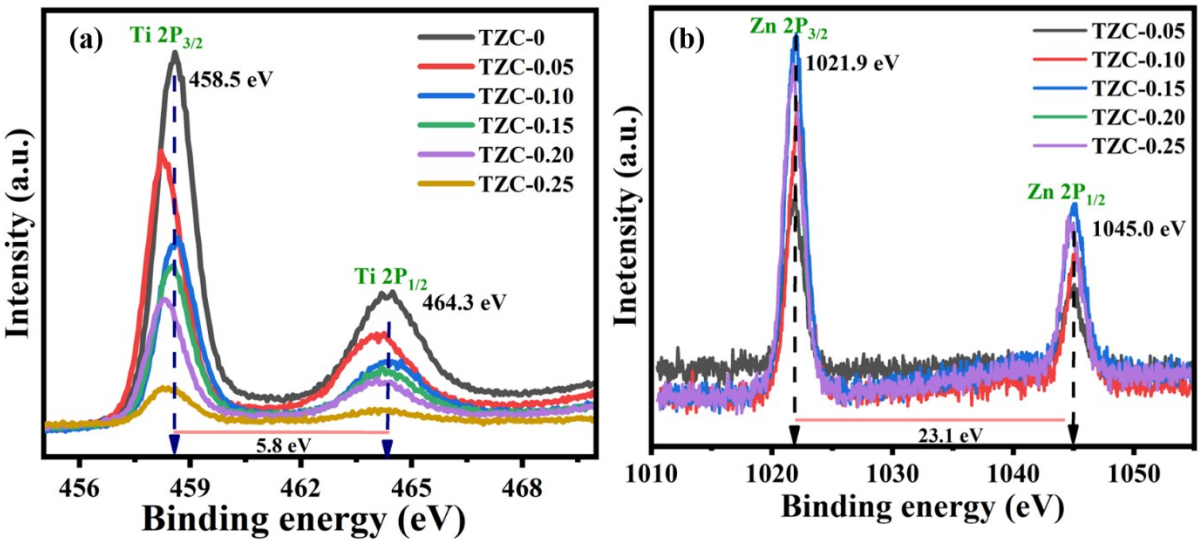

Fig S4: XPS core level spectra of (a) Ti 2p (b) Zn 2p spectra of mesosphere TiO_2 and TiO_2/ZnO nanocomposites.

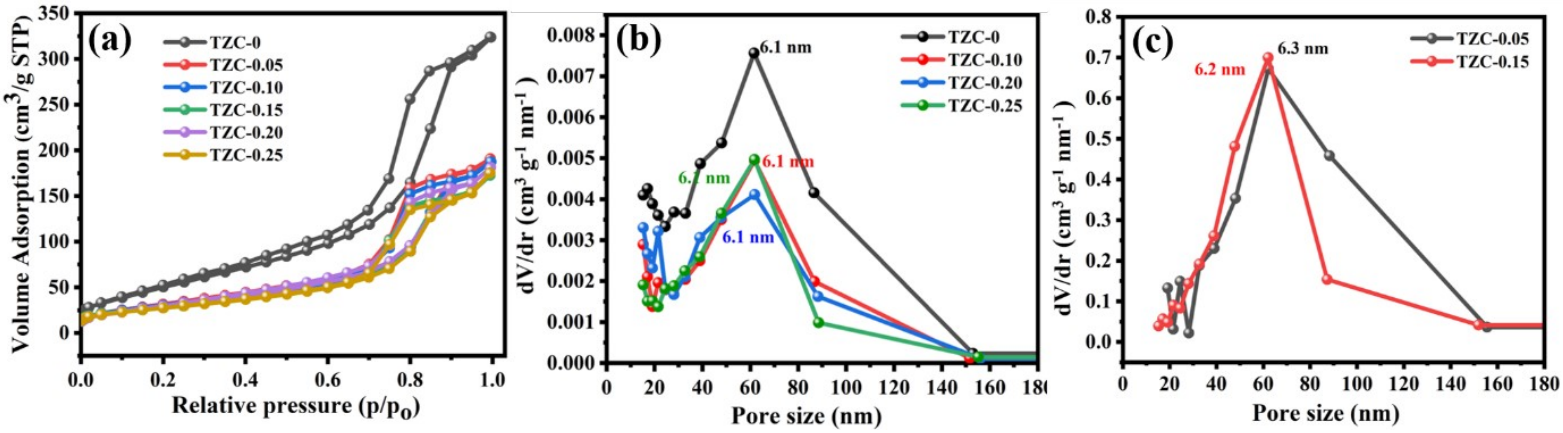

Fig S5: (a) BET surface areas and (b,c) pore size distributions of TZC-0, TZC-0.05, TZC-0.10, TZC-0.15, TZC-0.20, and TZC-0.25.

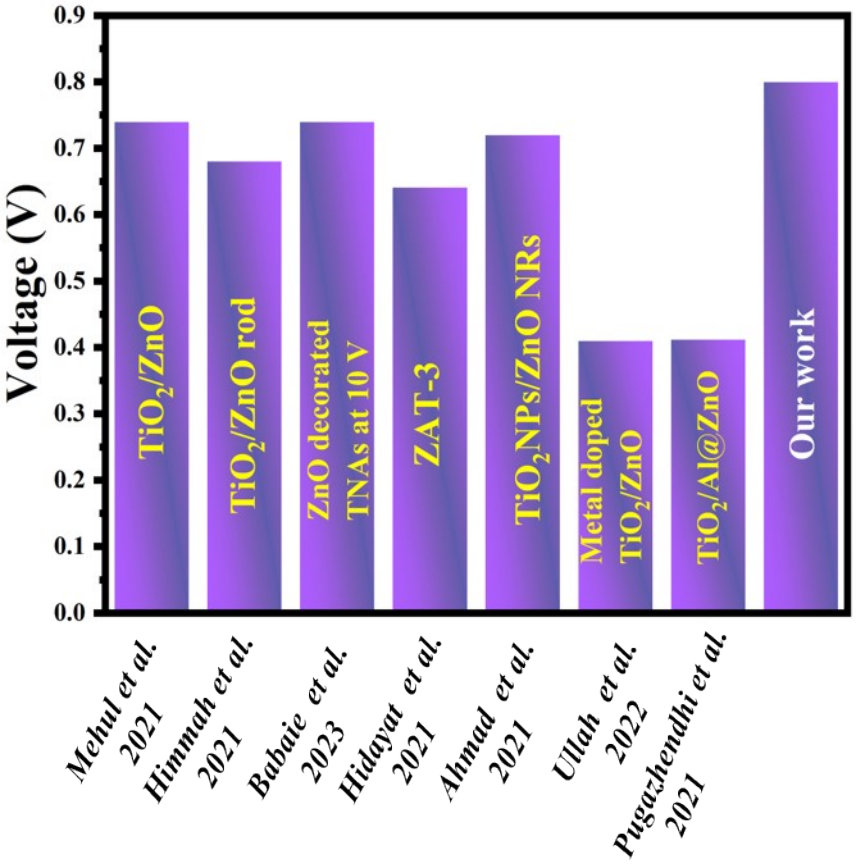

Fig S6: Comparison of best V_{OC} result with other reported results.

Sample Code	τ_1 (ps)	τ_2 (ps)	τ_2 (ps)	A_1	A_2	A_3
TZC-0	9.1×10^{-9}	3.1×10^{-10}	2.3×10^{-07}	9.1	46.6	44.1
TZC-0.05	8.5×10^{-9}	2.6×10^{-10}	2.2×10^{-07}	8.3	51.9	39.7
TZC-0.10	3.6×10^{-10}	1.0×10^{-08}	2.4×10^{-10}	41.7	9.6	48.6

Table S1: TRPL decay time of TZC-0, TZC-0.05, and TZC-0.10 samples.

Sample code	Surface area ($m^2\ g^{-1}$)	Pore volume (cc per g)	Pore diameter (nm)
TZC-0	166.3	0.48	6.1
TZC-0.05	110.5	0.28	6.3

TZC-0.10	104.2	0.28	6.1
TZC-0.15	103.7	0.26	6.2
TZC-0.20	105.8	0.27	6.1
TZC-0.25	95.1	0.27	6.1

Table S2: Parameters of surface area, pore volume and pore diameter of the mesosphere TiO_2 and TiO_2/ZnO nanocomposites.

Sample code	**R_s (ohm)**	**R_{ct1} (ohm)**	**R_{ct2} (ohm)**
TZC-0	30	125	51
TZC-0.05	30	54	43
TZC-0.10	25	73	60
TZC-0.15	40	189	105
TZC-0.20	43	137	240
TZC-0.25	1×10^3	100	10

Table S3: Performance parameter of EIS spectra with of TZC-0, TZC-0.05, TZC-0.10, TZC-0.15, TZC-0.20 and TZC-0.25 device are measured in dark condition.